ADVANCED FUNCTIONAL MATERIALS

FULL PAPER

Chain-Length Dependence of Singlet and Triplet Exciton Formation Rates in Organic Light-Emitting Diodes**

By *David Beljonne*, *Aijun Ye*, *Zhigang Shuai*, and *Jean-Luc Brédas**

The operation and efficiencies of molecular or polymer organic light-emitting diodes depend on the nature of the excited species that are formed. The lowest singlet and triplet excitons display different characteristics that impact on the quantum yields achievable in the devices. Here, by performing correlated quantum-chemical calculations that account for both the electronic couplings and energetics of the charge-recombination process from a pair of positive and negative polarons into singlet and triplet excitons, we show that the formation rates for singlet over triplet excitons vary with chain length and favor singlet excitons in longer chains. Thus, in polymer devices, the resulting singlet/triplet fraction can significantly exceed the spin-statistical limit.

1. Introduction

The design and fabrication of organic light-emitting diodes (LEDs) have attracted major interest worldwide because of the potential for applications of polymer-based devices in large-area flexible-display technology.[1–5] Light emission in such devices comes from the radiative decay of singlet excitations that are generated through recombination of charge carriers within the organic layer; in materials with small spin-orbit coupling, triplet excitations act as luminescence quenchers.

Primary excitations in these materials are generally believed to be excitons with a binding energy in excess of kT.[6] As a result of electron–phonon and electron–electron interactions, the lowest singlet (S_1) and triplet (T_1) excitons possess both different energies (the S_1–T_1 energy difference; the exchange energy K, is estimated to be ≥ 0.5 eV for the lowest excitations in a variety of conjugated polymers[7–9]) and different spatial wavefunctions (with T_1 displaying a more spatially confined character).[10] These marked differences have a major impact on the theoretical upper limit for the quantum yields achievable in organic LEDs.

The quantum efficiency for electroluminescence (EL) (photoluminescence (PL)), η_{EL} (η_{PL}), is defined as the ratio between the number of photons coming out of the device and the number of injected electrons (absorbed photons). The ratio η_{EL}/η_{PL} is controlled by the fraction of singlet excitons generated in the diode (hereafter referred to as η_2). It has long been thought to conform to simple spin-multiplicity rules; in this case, η_{EL}/η_{PL} does not exceed 25 % since the recombination of a pair of injected electron and hole (both spin 1/2) leads to four microstates with three triplet states and one singlet state. Recent experimental investigations, based on reverse-bias measurements of photoluminescence efficiencies, seem to support the view that η_2 is close to 20 % in both Alq_3 (a model molecular system) and poly[2-methoxy-5-(2-ethylhexyloxy)-1,4-phenylenevinylene] (MEH-PPV) (a model polymer material).[11] In contrast to that, there is compelling experimental[12–19] and theoretical[20–24] evidence that, in small conjugated oligomers and molecules,[18] η_2 follows spin statistics closely while, in conjugated polymers, larger ratios between EL and PL quantum yields can be achieved.[19] This underscores the possibility of achieving high efficiency in polymer-based LEDs (with quantum yields approaching unity) and raises fundamental questions about the mechanisms of exciton formation. Note that the large splitting between the lowest singlet and triplet excitons in conjugated polymers (on the order of 0.7 eV in phenylene-based materials)[7] largely prevents any contribution to the luminescence from thermalized triplet excitons.[25]

Charge recombination appears to occur as a two-step process.[19] First, initially free polarons (the injected charges) coalesce into bound singlet or triplet polaron pairs, also referred to as charge-transfer (CT) excitons; these intermediate states then decay into lower singlet or triplet exciton neutral states. A

[*] Prof. J.-L. Brédas, Dr. D. Beljonne, Dr. A. Ye, Prof. Z. Shuai
Chemistry of Novel Materials, University of Mons-Hainaut
Place du Parc 20, B-7000 Mons (Belgium)
E-mail: jean-luc.bredas@chemistry.gatech.edu
Prof. J.-L. Brédas
School of Chemistry and Biochemistry, Georgia Institute of Technology
Atlanta, GA 30332-0400 (USA)
Prof. Z. Shuai
Center for Molecular Science, Institute of Chemistry
The Chinese Academy of Sciences
Beijing 100080 (P.R. China)

[**] The authors are most grateful to Neil Greenham and Sir Richard Friend for stimulating discussions. This material is based upon work supported at Georgia Tech in part by the National Science Foundation through the STC Program under Award Number DMR-0120967 and through grant CHE-0342321, the Office of Naval Research, and the IBM Shared University Research Program. The work in Mons is partly supported by the European Commission IST program 'STEPLED', the Belgian Federal Services for Scientific, Technical, and Cultural Affairs (InterUniversity Attraction Pole 5/3) and the Belgian National Science Foundation (FNRS). The work in Beijing is supported by the National Science Foundation of China (Grant No. 90203015) and the Ministry of Science and Technology of China (973 programme Grant No. 2002CB613406). David Beljonne is an FNRS Senior Research Associate.

  DOI: 10.1002/adfm.200305176

ADVANCED FUNCTIONAL MATERIALS

major aspect to emphasize is that, when the second step is faster than any other process affecting the intermediate states, spin statistics is obeyed. Overcoming spin statistics requires that the second step be significantly slower for triplet than for singlet CT states. Then, one of two things can happen. Intersystem crossing can switch triplet pairs into singlet pairs[26] that will quickly decay down the singlet-exciton manifold; or, triplet pairs can have time to dissociate and some of the freed polarons can later re-associate as singlet pairs.

We have previously developed a theoretical model[20] to describe intermolecular charge recombination in conjugated materials, which includes both one- and two-electron contributions to the cross-sections as in reference [22]; the initial and final states were treated at the single configuration interaction level, which allowed the extension of the calculations to long chains, while keeping the salient features of the excited states. However, the chain-length dependence of the cross-sections was not addressed specifically and constitutes the main motivation for the present work.

Here, importantly, the electronic couplings and energetics of the charge-recombination process from polaron pairs to neutral excitons are both accounted for by applying the Jortner formulation for the calculation of charge-recombination rates;[27] see the Methodology section. Investigating model poly(*para*-phenylene vinylene) chains, we find that the formation rates of singlet over triplet neutral excitons vary with chain length and favor singlets in longer chains.

A likely scenario for the formation of the lowest exciton neutral states, S_1 and T_1, involves the following sequence: first, generation of bound charge-transfer ^{1}CT and ^{3}CT pairs that are amenable to intersystem crossing or dissociation; then, spin-dependent recombination into S_n and T_n exciton states, whose relative rates depend on the interplay between the electronic couplings and the spectral overlaps; and, finally, decay down the singlet and triplet manifolds to reach S_1 or T_1.

Here, we focus on the spin-dependent recombination process, which is believed to be the rate-limiting step in the exciton-formation mechanism. However, we stress that the overall rate for exciton generation could also be affected by the decay down the singlet and triplet manifolds, which is expected to favor the singlet versus the triplet route; in comparison to S_1, the formation of T_1 requires a larger amount of energy (i.e., the exchange energy K), to be dissipated under the form of vibrations; this has been shown to be detrimental to the resulting formation rate.[22]

2. Results and Discussion

We have considered two configurations, cofacial and head-to-tail, shown at the top of Figures 1,2 and calculated the electronic matrix elements, V_{if}, for charge recombination into both the singlet and triplet manifolds. The calculations were performed on oligomers ranging in size from 2 to 10 phenylene rings; hereafter, we only refer to the results obtained for phenyl-capped phenylene vinylene oligomers containing two rings,

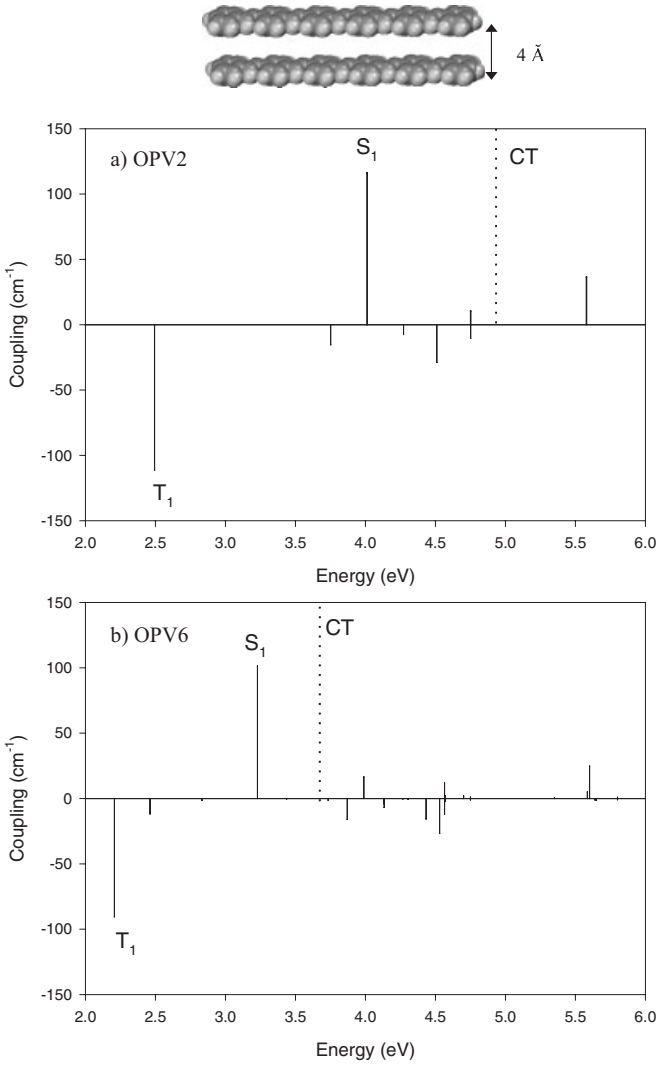

Figure 1. Charge-recombination electronic couplings, V_{if}, into singlet and triplet excited states in cofacial dimers of OPV2 (a) and OPV6 (b) molecules. For the sake of clarity, V_{if} values are reported as positive and negative values for singlets and triplets, respectively. The PPP/SCI excitation energies from the singlet ground state to the lowest singlet and triplet excited states are shown on the abscissa axis. The approximate energetic position of the lowest charge-separated state, as obtained from AM1/CI/COSMO calculations, is indicated by the dashed line. The molecular packing is shown at the top.

OPV2 (the *trans*-stilbene molecule) and six rings, OPV6; these are taken as representatives for 'small molecules' and 'polymer chains', respectively. In addition, only electron transfer from the charge-separated state to the exciton states is addressed here; similar results are obtained for hole hopping and will not be described. Figures 1,2 show the electronic couplings (tunneling matrix elements) for forming singlet and triplet excitons as a function of excitation energy in the cofacial and head-to-tail two-chain configurations, respectively. The evolution with chain length of the ratio between the electronic couplings into S_1 and T_1 is displayed in Figure 3. These results call for the following comments:

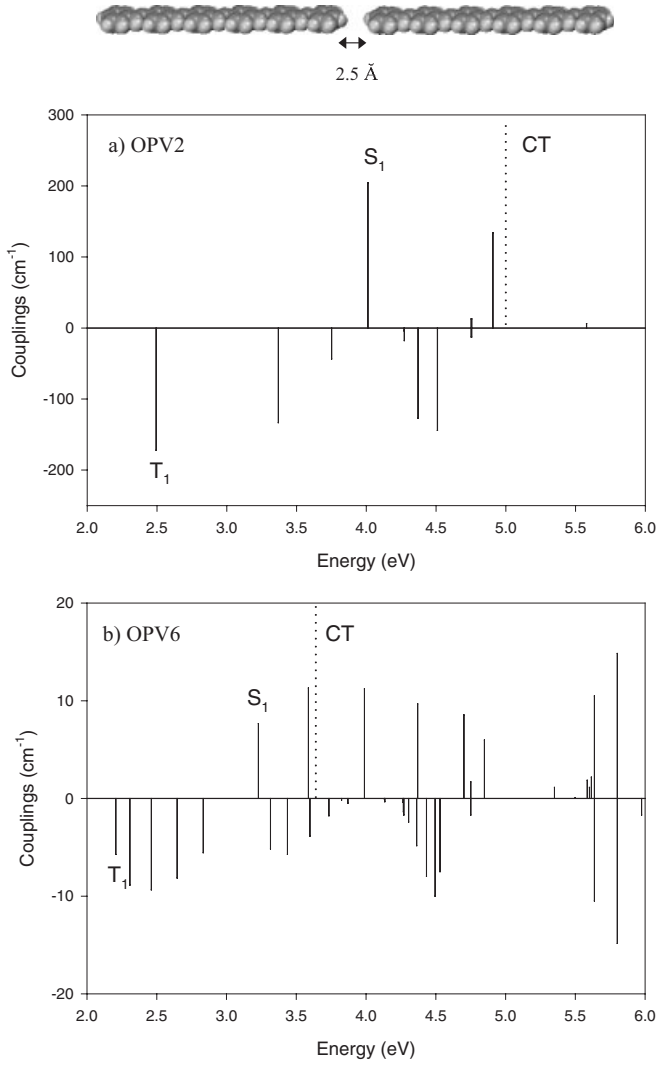

Figure 2. Charge-recombination electronic couplings, V_{if}, into singlet and triplet excited states in head-to-tail dimers of OPV2 (a) and OPV6 (b) molecules. Note the change in scale for the couplings (by a factor of 15) between (a) and (b). The molecular packing is shown at the top.

In the cofacial arrangements, the largest matrix elements are calculated for the lowest singlet S_1 and triplet T_1 excited states, in agreement with previous works.[20,23] This feature can be readily explained on the basis of the overlap between the wavefunctions of the initial and final states. Since the initial charge-transfer state is assumed to be a pure transition from the highest occupied molecular orbital (HOMO) of one chain to the lowest unoccupied molecular orbital (LUMO) of the other chain, optimal overlap is achieved with the final excited state that involves the largest contributions from these frontier orbitals, i.e., the lowest-lying singlet and triplet states. Note that the system in the cofacial arrangement possesses C_{2h} symmetry; only B_u-symmetry excited states are then allowed to couple electronically to the B_u-symmetry CT state.

The situation is somewhat different for the head-to-tail configurations, where a number of different singlet and triplet excited states show significant electronic couplings to the

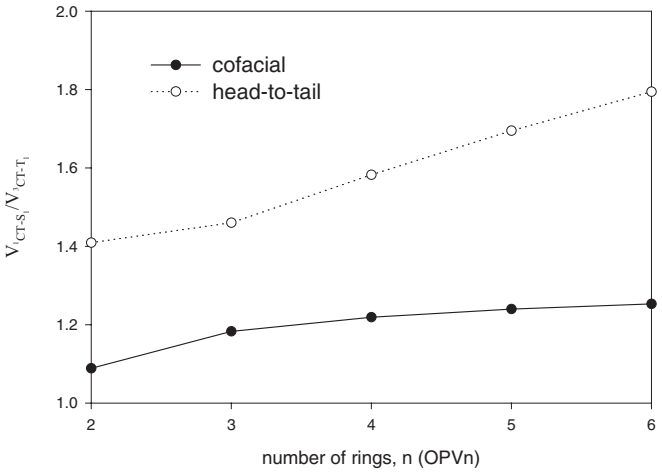

Figure 3. Evolution with chain length of the ratio between the exciton formation electronic couplings, V_{if}, into the lowest singlet and triplet excited states, in cofacial (solid line) and head-to-tail (dashed line) configurations.

charge-transfer state; this is partly due to the reduced symmetry of the head-to-tail arrangement. Here, chain-end contributions to the wavefunctions play a major role. From the calculated two-particle wavefunctions,[28] we found a clear correlation between the magnitude of the interchain matrix elements and the shape of the excited-state wavefunctions, more delocalized excited states leading to larger couplings.

While in cofacial aggregates the ratio between the matrix elements for charge recombination to yield S_1 versus T_1 is hardly chain-length dependent, the corresponding ratio shows a marked increase in the case of head-to-tail arrangements. This stems from the different nature of the lowest singlet and triplet excited states, the latter being more localized around the central part of the chain.[10] As expected, the differences in the spatial confinements of the S_1 and T_1 wavefunctions are amplified in the head-to-tail configurations for which contributions at the edges of the conjugated segments are the most relevant.

Electronic excitations in phenylene-based materials can be classified into three categories, depending on the nature of the involved molecular orbitals (MOs):[29,30] d–d* excitations, built by promoting an electron from an occupied delocalized MO to an empty delocalized MO; l–l* excitations, involving only orbitals that are localized on the phenylene rings; and d–l*/l–d* excitations, which correspond to transitions from occupied delocalized orbitals to unoccupied localized orbitals and vice versa. We first focus on the cofacial aggregates. Figure 1 indicates that there is a bunch of excited states, lying about 4.0–5.0 eV above the ground state, with recombination matrix elements on the order 10–30 cm^{-1}; in this spectral range, singlet and triplet excited states show similar electronic couplings, though slightly larger for the triplets. These high-lying excited states are assigned mainly to mixed d–l*/l–d* and, to a lesser extent, l–l* type excitations. Because of their reduced electron–hole overlap, the singlet and triplet d–l*/l–d* excited states are almost degenerate, display similar wavefunctions, and hence lead

ADVANCED FUNCTIONAL MATERIALS

to nearly equal charge-recombination cross-sections. As described below, these states could play an important role in the exciton formation mechanism in small molecules. In head-to-tail configurations (Fig. 2), the situation is more complex (note the differences in the scale of the electronic couplings between Figs. 1 and 2); higher-lying d–d* excitations acquire significant coupling with the charge-transfer state as a result of the lower symmetry of the dimers and close contacts between the edges of the conjugated segments (vide supra). It should be noted that the magnitude of the electronic couplings drops much more quickly with chain length in head-to-tail versus cofacial dimers, a feature that has also been underlined in the case of exciton energy-transfer processes.[31]

We now turn to the discussion of the driving force for the charge recombination reaction. In Figure 4, a schematic energy diagram with the relevant electronic states, as obtained from

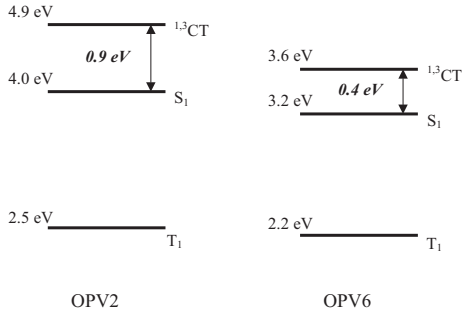

Figure 4. Schematic energy diagram showing the position of the lowest on-chain singlet, S_1, and triplet, T_1, excited states and the lowest charge-separated state, ^{1}CT, in a cofacial stack of OPV2 (a) and OPV6 (b) dimers.

AM1/CI/COSMO calculations (see Methodology), is presented for the cofacial OPV2 and OPV6 model dimers (assuming a distance between the molecular planes of 4 Å). In both cases, we find that the lowest intrachain singlet excited state lies below the charge-separated state. This supports the view that primary photoexcitations in PPV are on-chain excitations and not polaron pairs.[32] However, the most important result is that the energy difference Δ_S between S_1 and ^{1}CT decreases significantly when going from OPV2 ($\Delta_S \sim 0.9$ eV) to OPV6 ($\Delta_S \sim 0.4$ eV). Such an evolution is consistent with recent experimental investigations by Bässler and co-workers;[33] the results suggest that the origin of the delayed fluorescence observed in highly ordered ladder-type poly(*para*-phenylene) comes from the recombination of geminate electron–hole pair states into intrachain emissive excitons, implying an energy difference between the two species on the order of kT.

Although we have not performed any detailed calculations of the reorganization energy, we can estimate its magnitude. The inner part, λ_i, corresponds to the energy required to switch from the geometry of two oppositely charged polarons (forming the charge-separated state) to the equilibrium geometry of the target excited state on one chain and the ground-state geometry on the other chain. Due to the similarity in geometric distortions induced by charge injection or neutral excitation in a conjugated chain (at least for the lowest singlet excited state),[34] this contribution is expected to be on the order of the polaron relaxation energy. We have therefore chosen a λ_i value of ~0.15 eV, which together with an effective vibrational mode of 0.15 eV leads to a Huang–Rhys factor $S \sim 1$. Because of the low dielectric constant of organics and the short separation between the positive and negative charges in the charge-transfer state, the medium contribution to the relaxation energy ought also to be small, on the order of that found in weakly polar media (typically a few tenths of an electronvolt).

From this discussion, it is clear that the approximations considered here prevent quantitative predictions of the exciton formation rates. To make sure that our choice of molecular parameters does not affect the overall picture, we have applied Equation 1 (see Methodology below) to a range of λ_s and Δ_S values (chosen for the latter around the calculated AM1 values). The resulting ratios between singlet and triplet exciton generation rates, $r = k_S/k_T$, are reported as two-dimensional grids in Figures 5,6, for the two model systems and molecular arrangements considered in this work. As expected, the absolute values of the rates are very sensitive to the relative magnitude of the driving force with respect to the reorganization energy (which according to the classical view sets the height of the barrier for the recombination reaction). However, the important results are the following. First, for most of the $\{\lambda_s,\Delta_S\}$ space explored, the k_S/k_T ratio is smaller or close to one in OPV2 while it is much higher in OPV6 (especially in the cofacial configuration). Second, in spite of the relatively small electronic couplings, the calculated recombination rates at room temperature are relatively fast (they somewhat vary as a function of the actual values chosen for the reorganization energy and driving force): in OPV2, on the order of 10^9–10^{10} s^{-1} for both singlets and triplets; in OPV6, ca. 10^{10}–10^{11} for singlets but significantly smaller, 10^7–10^8, for triplets.

These results can be understood in the following way. For small molecules in a face-to-face arrangement, the rather large energy separation between the charge-separated state and the lowest singlet excited state reduces the efficiency of the direct S_1 generation. In this case, higher-lying singlet S_n states, closer in energy and electronically coupled to the initial charge-transfer state, are formed with a higher probability; these include the d–l*/l–d* excitations described above. Since these excited states are only weakly split by exchange interactions, the corresponding triplet T_n excited states have comparable excitation energies, wavefunctions, electronic couplings, and therefore recombination rates. It follows that, in short oligomers, singlets and triplets form with comparable probabilities and spin statistics are pretty much obeyed. In contrast, the S_1 pathway is dominant in long chains due to the reduced S_1–^{1}CT energy gap and the larger tunneling matrix element associated with that state. Since S_1 shows the largest electronic coupling, the singlet route is favored over the triplet channel in extended systems; this results in ratios between singlet and triplet formation rates largely exceeding one. The situation is again more complex in head-to-tail arrangements where higher-lying d–d* excited

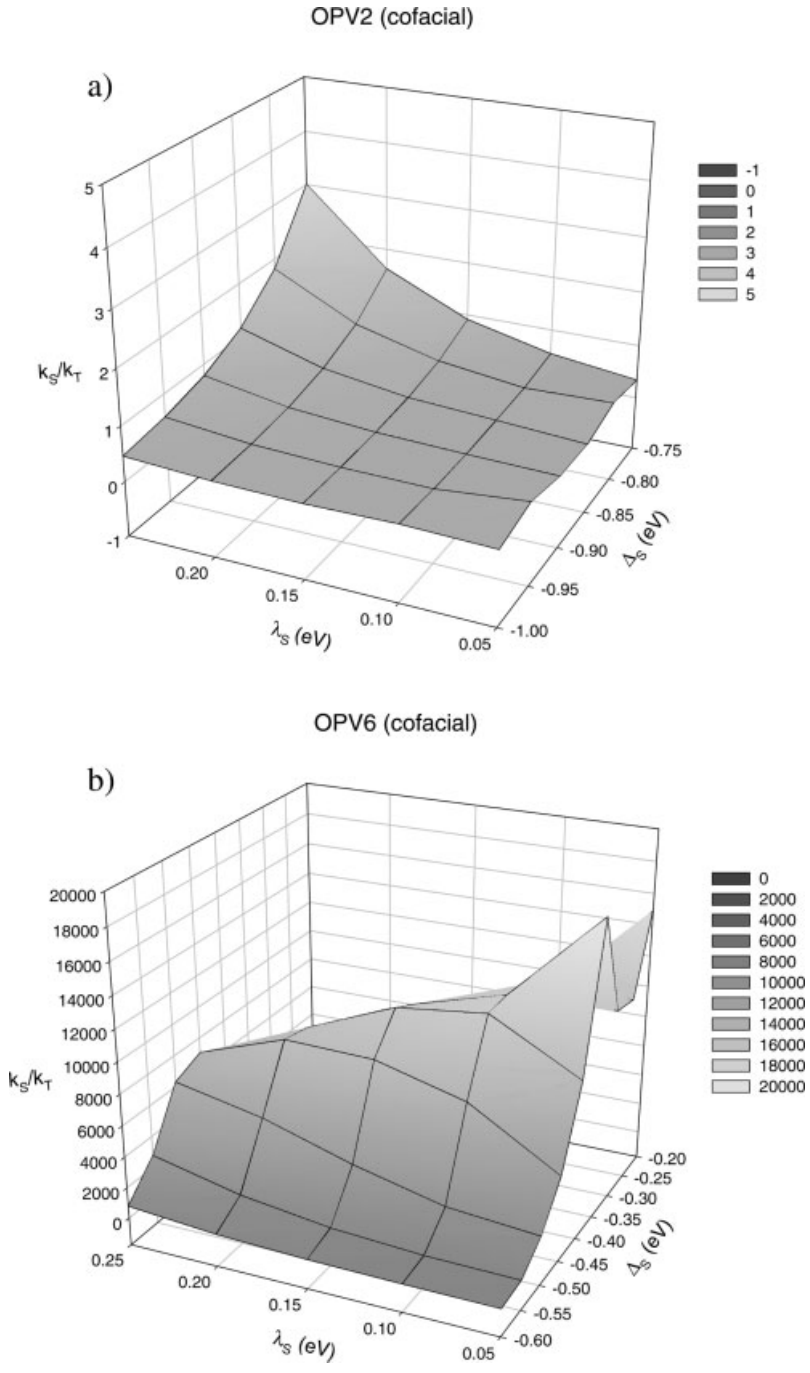

Figure 5. Ratio between the singlet and triplet charge-recombination rates, $r = k_S/k_T$, as a function of Δ_S and λ_S, in a cofacial arrangement of two OPV2 (a) and OPV6 (b) chains. The rate constants have not been weighted by spin distribution.

states also play a significant role. We stress that, in all cases, direct formation of T_1 is very unlikely due to the very large change in Gibbs' free energy (on the order of 1.5 eV in OPV6 and larger than 2 eV in OPV2), which sets this process into the inverted Marcus region.[35] (At this stage, it is useful to point out that the absolute values of the matrix elements for electron–hole recombination do depend on the actual geometric configurations—which are expected in reality to be less ideal than those considered here. However, fluctuations in the contacts between the molecules will not significantly affect the overall conclusions discussed above. Indeed, the main source for the chain-length dependence of the singlet over triplet exciton formation rates is the energy mismatch between the initial and final electronic states, which is mostly driven by conjugation length.)

While the mechanism proposed above specifically applies to phenylene-based materials (for which different types of excitations are encountered), our results can be generalized to a number of other conjugated polymers. Indeed, in the simplest one-dimensional two-band model (such as the one used to describe the excited states in polyenes),[36] the average electron–hole separation of the on-chain excitations goes up with increasing energy. Hence, high-lying excited states are less subject to exchange interactions, which decay exponentially with distance. Since it can be reasonably expected that only these higher-energy states are reached efficiently in small molecules or oligomers, this will result in singlet and triplet formation rates of comparable magnitudes. In extended π-systems, contributions from the lowest excited state should dominate the mechanism of singlet generation, because of both large electronic recombination matrix elements and small energy barriers. This process is expected to occur at a faster rate than the formation of any triplet T_n excited state; hence, triplets should be created at a lower rate than singlets, opening the way to deviations from spin statistics.

Finally, we address the dependence of r on the material. Using transient-spectroscopic techniques, Wohlgenannt et al. have measured the formation cross-section ratio r of singlet and triplet excitons in a variety of π-conjugated materials. They found that the larger the conjugation length, the higher the singlet population.[16] If one assumes comparable exchange energies for the systems investigated (which is consistent with a number of experimental data[7] and the results of single-configuration interaction calculations),[37] the deciding factor is then the energy separation between the charge-separated state (with the charges either far apart on the same chain or in a two-chain polaron pair configuration) and the lowest singlet exciton. The experimental data from the literature[15] indicate that r increases in the following sequence: sexithienyl < poly(*para*-phenylene ethynylene) < poly(*para*-phenylene vinylene) < regio-random poly(hexylthiophene) < ladder-type poly(*para*-phenylene) (mLPPP) < regio-regular poly(hexylthiophene)

ADVANCED FUNCTIONAL MATERIALS

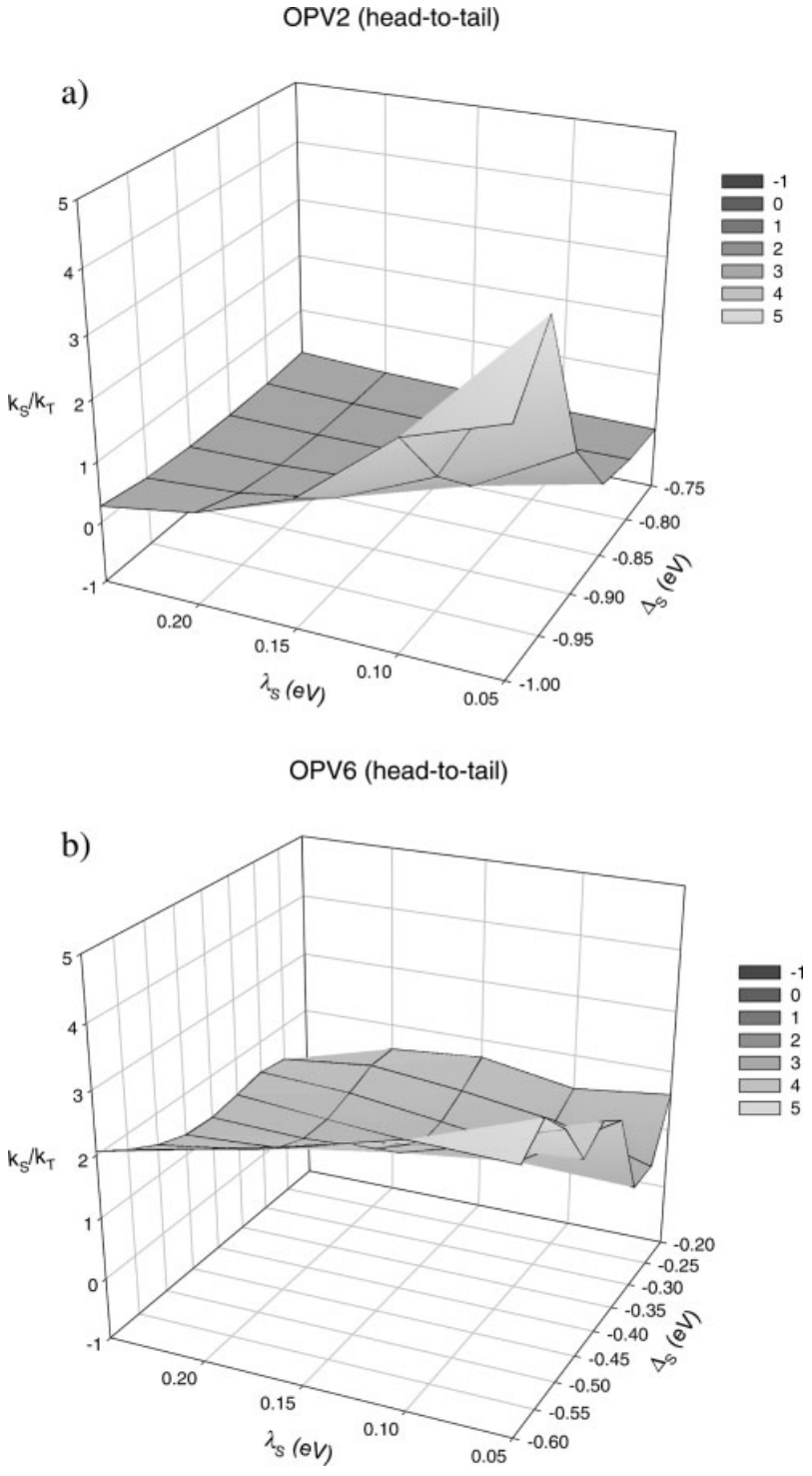

Figure 6. Ratio between the singlet and triplet charge-recombination rates, $r = k_S/k_T$, as a function of Δ_S and λ_S, in a head-to-tail arrangement of two OPV2 (a) and OPV6 (b) chains. The rate constants have not been weighted by spin distribution.

(RR-P3HT). These trends are consistent with material-dependent Δ_S values (i.e., the energy separation between S_1 and the lowest charge-transfer or polaron-pair state); Δ_S is very sensitive not only to the chemical structure of the individual conjugated chains but also most importantly to the way these chains pack in the solid state, with the lowest values found in the most highly ordered materials (due to shorter average electron–hole separation in the CT pair). The largest ratios between singlet and triplet yields measured for RR-P3HT and mLPPP confirm the hypothesis that small Δ_S values (these two materials display a high degree of both intrachain and interchain order) translate into efficient singlet generation and r values largely exceeding one.

3. Conclusions

In summary, we have explored the mechanisms of singlet- and triplet-exciton formation in electroluminescent π-conjugated materials. Model calculations, based on electron-transfer theory, have been performed on systems made of two phenylenevinylene oligomers of increasing size, arranged in either a cofacial or head-to-tail configuration. The main conclusions from our work are as follows:

- Deviations from simple spin statistics (according to which only one quarter of excitons are formed as singlets) occur if triplet CT excitons (polaron pairs) are amenable to intersystem crossing or dissociation.
- The electronic couplings between the charge-separated state and the neutral exciton state are predicted to be largest for S_1 and T_1. However, because of the large exchange energy K (S_1–T_1 energy difference), the probability for direct recombination into T_1 is, in all cases, vanishingly small (Marcus inverted regime).
- In small molecules, the CT–S_1 energy difference is large. Formation of both singlet and triplet excitons proceeds via higher-lying S_n/T_n states, which display similar electronic couplings and are therefore characterized by similar formation rates. These rates are fast and, as a result, spin statistics are expected to be obeyed.
- In extended conjugated chains, the energy difference between the CT and S_1 excited states becomes on the order of the reorganization energy (i.e., a few tenths of an electronvolt) and the $^1CT \rightarrow S_1$ pathway tends to be even faster than in small molecules. In contrast, the $^3CT \rightarrow T_n$ channel becomes slower, leaving room for intersystem crossing or dissociation.

In a simplified picture, these results imply that the smaller the energy separation between the charge-separated state and the lowest singlet-exciton state, the higher the relative generation of singlets versus triplets. This model is consistent with the

material-dependent singlet/triplet fractions that have recently been reported.[16] Further work is in progress to confirm the general character of these conclusions.

Finally, a comment is in order on the implications of our results for the design of novel conjugated polymer materials with enhanced electroluminescence quantum yields. If the deciding factor in the efficiency of singlet versus triplet exciton generation is the energy difference between the lowest intermolecular charge-separated state and the S_1 exciton state, it follows that highly ordered materials (with short intermolecular contacts and delocalized charges) should have the largest singlet/triplet ratios. However, this does not necessarily imply that the highest quantum yields can be reached. Indeed, by reducing the energy separation between intrachain and interchain excitations, the relative population of non-emissive polaron pair species should also increase, which could potentially impact the balance between radiative and non-radiative decay channels. Thus, there is a need to develop materials where an optimal compromise can be achieved between singlet exciton generation and luminescence efficiency.

4. Methodology

In the case of charge-recombination (CR) processes, the semi-classical expression for the CR rate writes, within the Franck–Condon approximation and the displaced harmonic oscillator model, as:[27]

$$k_{CR} = \frac{2\pi}{\hbar} \left| < \psi_0 \left| W \right| \psi_f > \right|^2 \left(\frac{1}{4\pi\lambda_s kT} \right)^{1/2} \sum_v e^{-S} \frac{S^v}{v!} \exp\left(- \frac{(\Delta G^0 + \lambda_s + v\hbar\langle\omega_i\rangle)^2}{4\lambda_s kT} \right) \quad (1)$$

where ψ_0 and ψ_f denote the wavefunctions of the initial (charge-separated) state and final (singlet- and triplet-exciton) state, respectively; W is the perturbation; λ_s denotes the external (medium) reorganization energy induced by the electron transfer; ΔG^0 is the variation in Gibbs' free energy during the reaction; and S is the Huang–Rhys factor expressed in terms of the inner reorganization energy λ_i and the energy of an effective vibrational mode $\hbar\langle\omega_i\rangle$:

$$S = \frac{\lambda_i}{\hbar\langle\omega_i\rangle} \quad (2)$$

The inner reorganization energy (λ_i) corresponds to the energy required to accommodate the nuclear rearrangements occurring upon charge transfer when going from the equilibrium geometry of the initial state to that of the final state. Here, λ_i and λ_s were taken as free parameters. For charge recombination, the Gibbs' free energy is the energy difference between the initial charge-separated state and the final exciton state, which needs to be defined for both the singlet and triplet pathways.

Singlet and triplet excited-state energies were obtained by combining a Pariser–Parr–Pople (PPP) Hamiltonian with a single-configuration interaction (SCI) scheme. Standard parameters have been used for transfer and on-site repulsion integrals[20] and the Ohno–Klopman potential[38] has been adopted to depict electron–electron interactions. The relative position of the charge-transfer state with respect to the lowest singlet exciton state has been modeled as follows. The equilibrium geometries of isolated chains carrying either a positive or a negative charge were first optimized at the AM1[39] level; the relaxed geometries in the lowest singlet excited state were obtained from AM1/CI calculations (the active space in the configuration interaction calculations was increased with increasing molecular size, to ensure size consistency). To account for polarization effects induced by the medium, the energies of the excitonic and polaronic species were computed within the continuum dielectric approximation through the use of the COSMO model[40] implemented in AMPAC.[41] Finally, the initial state in the recombination process, which in our model corresponds to a pair of opposite charges lying on adjacent conjugated segments, is further stabilized by Coulomb interactions; this energy shift can be estimated on the basis of the AM1/Mulliken atomic charge distributions in the positive and negative polarons:

$$E_{cb} = \frac{1}{4\pi\varepsilon_0} \sum_i \sum_j \frac{q_i q_j}{\varepsilon r_{ij}} \quad (3)$$

where, q_i [q_j] is the charge on site i [j] in the positively [negatively] charged chain and r_{ij} the distance between sites i and j; ε is the medium dielectric constant, which is taken both in Equation 3 and the COSMO calculations to be equal to four, a typical value for the dielectric constant of organic conjugated polymers.[42,43] The energy separation between the initial charge-separated state and the lowest excited state for the singlet process then writes:

$$\Delta_S = \{E(P^{+\bullet}) + E(P^{-\bullet}) - 2 \times E(S_0) + E_{cb}\} - E(S_1) \quad (4)$$

where the first four terms on the right refer to the energy of the charge-separated state; $E(P^+)$, $E(P^-)$, $E(S_0)$, and $E(S_1)$ correspond to the energies, in their relaxed geometries, of the positive and negative polarons and the singlet ground and excited states, respectively. Note that Δ_S is the driving force, ΔG^0, for the charge recombination reaction into S_1; the changes in Gibbs' free energy relative to the processes yielding higher-lying singlet S_n states or triplet T_n excited states are obtained by adding to Δ_S the S_n–S_1 or T_n–S_1 energy difference as provided by the PPP/SCI scheme (for such processes, the entropy effects can be neglected).

The electronic matrix elements (couplings), $V_{0f} = \langle\psi_0 \left| W \right| \psi_f\rangle$, for tunneling from the initial charge-separated state to the final exciton state were computed from first-order perturbation theory using the PPP/SCI excited states of the isolated molecules

ADVANCED FUNCTIONAL MATERIALS

as the zeroth-order wavefunctions and the interactions between the conjugated segments as the perturbation,[20] i.e., for electron transfer from segment 2 to segment 1:

$$V_{0f} = < \mathrm{CT}^{1,3} \left| H \right| \mathrm{ex}^{1,3} > \tag{5}$$

$$\left|\mathrm{CT}^{1,3}\right\rangle = \frac{1}{\sqrt{2}}(\mathrm{L}^{+}_{2\uparrow}\mathrm{H}_{1\uparrow} \pm \mathrm{L}^{+}_{2\downarrow}\mathrm{H}_{1\downarrow})\left|\mathrm{HF\text{-}SCF}\right\rangle$$

$$\left|\mathrm{ex}^{1,3}\right\rangle = \frac{1}{\sqrt{2}}\sum_{i_1 a_1} Z_{\mathrm{i}_1\mathrm{a}_1}(a^{+}_{1\uparrow} i_{1\uparrow} \pm a^{+}_{1\downarrow} i_{1\downarrow})\left|\mathrm{HF\text{-}SCF}\right\rangle$$

$$H' = \sum_{pq} h_{\mathrm{pq}} p^{+} q + \frac{1}{4}\sum_{pqrs} < \mathrm{pq}\|\mathrm{rs} > p^{+} q^{+} sr$$

where $\left|\mathrm{CT}\right\rangle$ and $\left|\mathrm{ex}\right\rangle$ denote the charge-separated and exciton states, respectively (1 and 3 denote the spin multiplicities, with associated + and – signs in the wavefunction expression, respectively). L_2 is the LUMO of segment 2, and H_2 the HOMO of segment 2, etc.; $\left|\mathrm{CT}\right\rangle$ as defined above then represents an initial state with an electron in segment 2 and a hole in segment 1. The coefficients Z in the expression of $\left|\mathrm{ex}\right\rangle$ denote the CI expansion coefficients for the excited-state wavefunctions; a^{+} and i correspond to creation and annihilation operators over MO a (unoccupied) and i (occupied), respectively (p^{+} and q are the corresponding operators for generic MOs p and q); $\left|\mathrm{HF\text{-}SCF}\right\rangle$ represents the electronic configuration of the Hartree–Fock self-consistent-field ground state; h_{pq} is the one-electron hopping integral, $t^{\perp}$, in the MO representation:

$$h_{\mathrm{pq}} = \sum_{\mu_1 \nu_2} t^{\perp}(\mu_1, \upsilon_2) C_{\mathrm{p}\mu_1} C_{\mathrm{q}\nu_2} \tag{6}$$

where $\langle \mathrm{aj}\|\mathrm{ib}\rangle = \langle \mathrm{aj}\,|\,\mathrm{ib}\rangle - \langle \mathrm{aj}\,|\,\mathrm{bi}\rangle$, $\langle \mathrm{aj}\,|\,\mathrm{ib}\rangle = [\mathrm{ai}\,|\,\mathrm{jb}]$, and

$$\langle pq \mid rs\rangle = \sum_{\mu\nu\sigma\tau} C_{\mathrm{p}\mu} C_{\mathrm{q}\nu} C_{\mathrm{r}\sigma} C_{\mathrm{s}\tau} [\mu\sigma|\nu\tau] \tag{7}$$

C is the linear combination of atomic orbitals (LCAO) coefficient of the one-electron wavefunction and $[\mu\sigma\,|\,\nu\tau]$ is the Coulomb integral in the site representation.

The use of an SCI approach has been validated through comparison to the results provided by more sophisticated CCSD (coupled cluster single and double) calculations.[44] As in reference [20], the initial state is modeled within a two-chain system and we take into account two possible orientations for the conjugated chains, see top of Figures 1,2. While 'interchain' electron or hole hopping between adjacent chains lying in a cofacial (or, more generally, H-type) arrangement is the most likely scenario in short chains, migration of the charges between conjugated segments on the same chain is also possible in longer (polymer) chains; the head-to-tail configuration in Figure 2 is intended to model such an 'intrachain' process. In order to ensure the general character of our results, we have only considered the simplest case of electron (hole) hopping between localized segments and ignored bond-charge correlation terms[20–23] (we actually anticipate that the effects described in the discussion section will be amplified when including such refinements). We consider the lowest-lying charge-transfer state as the initial state in the recombination process; this state is described by a single determinant built by promoting an electron from the HOMO of one chain to the LUMO of an adjacent chain. This is reasonable since the electron (hole) can relax from higher unoccupied (lower occupied) orbitals to the lowest (highest) one, prior to recombination. The wavefunctions for the exciton states are provided by a configuration interaction between all singly excited determinants built on the basis of the electronic structure of the isolated chains.

Received: December 10, 2003
Final version: February 4, 2004

[1] J. H. Burroughes, D. D. C. Bradley, A. Brown, R. N. Mackley, R. H. Friend, P. L. Burn, A. B. Holmes, *Nature* **1990**, *347*, 539.
[2] J. R. Sheats, H. Antoniadis, M. Hueschen, W. Leonard, J. Miller, R. Moon, D. Roitman, A. Stocking, *Science* **1996**, *273*, 884.
[3] R. H. Friend, R. W. Gymer, A. B. Holmes, J. H. Burroughes, R. N. Marks, C. Taliani, D. D. C. Bradley, D. A. Dos Santos, J. L. Bredas, M. Löglund, W. R. Salaneck, *Nature* **1999**, *397*, 121.
[4] A. H. Tullo, *Chem. Eng. News* **2000**, *78(26)*, 20.
[5] E. Grant, P. Nolan, D. Pinner, *The McKinsey Quarterly* **2002**, *1*, 18.
[6] N. S. Sariciftci, *Primary Photoexcitations in Conjugated Polymers: Molecular Exciton versus Semiconductor Band Model*, World Scientific, Singapore **1997**.
[7] A. Köhler, J. S. Wilson, R. H. Friend, M. K. Al-Suti, M. S. Khan, A. Gerhard, H. Bassler, *J. Chem. Phys.* **2002**, *116*, 9457.
[8] A. P. Monkman, H. D. Burrows, L. J. Hartwell, L. E. Horsburgh, I. Hamblett, S. Navaratnam, *Phys. Rev. Lett.* **2001**, *86*, 1358.
[9] D. Hertel, *Adv. Mater.* **2001**, *13*, 65.
[10] D. Beljonne, Z. Shuai, R. H. Friend, J. L. Brédas, *J. Chem. Phys.* **1995**, *102*, 2042.
[11] M. Segal, M. A. Baldo, R. J. Holmes, S. R. Forrest, Z. G. Soos, *Phys. Rev. B* **2003**, *68*, 075 211.
[12] Y. Cao, I. D. Parker, G. Yu, C. Zhang, A. J. Heeger, *Nature* **1999**, *397*, 414.
[13] P. K. H. Ho, J. S. Kim, J. H. Burroughes, H. Becker, S. F. Y. Li, T. M. Brown, F. Cacialli, R. H. Friend, *Nature* **2000**, *404*, 481.
[14] J. S. Wilson, A. S. Dhoot, A. J. A. B. Seeley, M. S. Khan, A. Kohler, R. H. Friend, *Nature* **2001**, *413*, 828.
[15] M. Wohlgenannt, K. Tandon, S. Mazumdar, S. Ramasesha, Z. V. Vardeny, *Nature* **2001**, *409*, 494.
[16] M. Wohlgenannt, X. M. Jiang, Z. V. Vardeny, R. A. J. Janssen, *Phys. Rev. Lett.* **2002**, *88*, 197 401.
[17] A. S. Dhoot, D. S. Ginger, D. Beljonne, Z. Shuai, N. C. Greenham, *Chem. Phys. Lett.* **2002**, *360*, 195.
[18] M. A. Baldo, D. F. O'Brien, M. E. Thompson, S. R. Forrest, *Phys. Rev. B* **1999**, *60*, 14 422.
[19] T. Virgili, G. Cerullo, L. Lüer, G. Lanzani, C. Gadermaier, D. D. C. Bradley, *Phys. Rev. Lett.* **2003**, *90*, 247 402.
[20] Z. Shuai, D. Beljonne, R. J. Silbey, J. L. Brédas, *Phys. Rev. Lett.* **2000**, *84*, 131.
[21] M. N. Kobrak, E. R. Bittner, *Phys. Rev. B* **2000**, *62*, 11 473.
[22] S. Karabunarliev, E. R. Bittner, *Phys. Rev. Lett.* **2003**, *90*, 057 402.
[23] K. Tandon, S. Ramasesha, S. Mazumdar, *Phys. Rev. B* **2003**, *67*, 045 109.
[24] T. Hong, H. Meng, *Phys. Rev. B* **2001**, *63*, 075 206.
[25] A. L. Burin, M. A. Ratner, *J. Chem. Phys.* **1998**, *109*, 6092.
[26] V. Dyakonov, G. Rösler, M. Schwoerer, E. L. Frankevich, *Phys. Rev. B* **1997**, *56*, 3852.
[27] J. Jortner, *J. Chem. Phys.* **1976**, *64*, 4860.

[28] Zoa v2.0, J. P. Calbert, Service de Chimie des Matériaux Nouveaux, University of Mons-Hainaut (Belgium); see, for instance, E. Zojer, A. Pogantsch, E. Hennebicq, D. Beljonne, J. L. Bredas, P. S. de Freitas, U. Scherf, E. J. W. List, *J. Chem. Phys.* **2002**, *117*, 6794.
[29] Y. N. Garstein, M. J. Rice, E. M. Conwell, *Phys. Rev. B* **1995**, *52*, 1683.
[30] A. Köhler, D. A. dos Santos, D. Beljonne, Z. Shuai, J.-L. Brédas, A. B. Holmes, A. Kraus, K. Müllen, R. H. Friend, *Nature* **1998**, *392*, 903.
[31] D. Beljonne, G. Pourtois, C. Silva, E. Hennebicq, L. M. Herz, R. H. Friend, G. D. Scholes, S. Setayesh, K. Müllen, J.-L. Bredas, *Proc. Natl. Acad. Sci. USA* **2002**, *99*, 10 982.
[32] N. T. Harrison, G. R. Hayes, R. T. Philipps, R. H. Friend, *Phys. Rev. Lett.* **1996**, *77*, 1881.
[33] D. Hertel, E. V. Soh, H. Bässler, L. J. Rothberg, *Chem. Phys. Lett.* **2002**, *361*, 99.
[34] J. L. Brédas, J. Cornil, A. J. Heeger, *Adv. Mater.* **1996**, *8*, 447.
[35] R. A. Marcus, *J. Chem. Phys.* **1965**, *43*, 679.
[36] See, for instance: D. Guo, S. Mazumdar, S. N. Dixit, F. Kajzar, F. Jarka, Y. Kawabe, N. Peyghambarian, *Phys. Rev. B* **1993**, *48*, 1433.
[37] A. Köhler, D. Beljonne, *Adv. Funct. Mater.* **2004**, *14*, 11.
[38] K. Ohno, *Theor. Chim. Acta* **1964**, *2*, 219; G. Klopman, *J. Am. Chem. Soc.* **1964**, *86*, 4550.
[39] M. J. S. Dewar, E. G. Zoebisch, E. F. Healy, J. J. P. Stewart, *J. Am. Chem. Soc.* **1985**, *107*, 3902.
[40] J. Tomasi, M. Persico, *Chem. Rev.* **1994**, *94*, 2027.
[41] Ampac 6.55 ed.; Semichem: 7204 Mullen, Shawnee, KS 66 216 (1997).
[42] D. Comoretto, G. Dellepiane, F. Marabelli, J. Cornil, D. A. dos Santos, J.-L. Bredas, D. Moses, *Phys. Rev. B* **2000**, *62*, 10 173.
[43] J.-W. van der Horst, P. A. Bobbert, P. H. L. de Jong, M. A. J. Michels, G. Brocks, P. J. Kelly, *Phys. Rev. B* **2000**, *61*, 15 817. According to these authors, it is the perpendicular dielectric constant that plays the dominant role in the interchain screening along the chain; a value of ~3 was calculated for that component.
[44] A. Ye, Z. Shuai, J. L. Brédas, *Phys. Rev. B* **2002**, *65*, 045 208.

